Tetrahedron 69 (2013) 4866–4874

Contents lists available at SciVerse ScienceDirect

Tetrahedron

journal homepage: www.elsevier.com/locate/tet

Azathia crown ether possessing a dansyl fluorophore moiety functionalized silica nanoparticles as hybrid material for mercury detection in aqueous medium

Jalal Isaad [a,b,*], Ahmida El Achari [a,b]

[a] University Lille Nord de France, F-5900 Lille, France
[b] ENSAIT, GEMTEX, F-59056 Roubaix, France

ARTICLE INFO

Article history:
Received 7 March 2013
Received in revised form 7 April 2013
Accepted 12 April 2013
Available online 19 April 2013

Keywords:
Magnetite
Silica
Nanoparticle
Mercury
Water
Hybrid material

ABSTRACT

A novel fluorescent hybrid material for Hg^{2+}detection using a derivative of dansyl fluorophore with azathia crown ether moiety grafted on silica nanoparticles (**SiNPs**) was prepared and characterized. The designed nanosensor exhibited pronounced Hg^{2+} selective ON–OFF type fluorescence switching upon binding. The presence of other metal ions has no observable effect on the sensitivity and selectivity of the prepared nanosensor toward the Hg^{2+} anions. The new nanosensor provided highly selective sensing to Hg^{2+}) in EtOH/water solvent mixtures (pH=7) with a detection limit of 10^{-7} M.

1. Introduction

Mercury is one of the most highly poisonous and hazardous pollutants with recognized accumulative and persistent characters in the environment and biota.[1–3] Inorganic mercury (Hg^{2+}) can be converted into methyl mercury by bacteria in the marine system and can easily enter the food chain and accumulate in the upper level, especially in large edible fish.[1–3] Mercury can cause serious human health problems including DNA damage, mitosis impairment, and permanent damage to the central nervous system.[4,5] To allow mercury detection with rapid, convenient, and inexpensive methods, a fluorescent sensor can be useful. A number of macromolecules have been proposed and prepared as new fluorescent sensors due to their high selectivity and sensitivity for the detection of metal cations, including mercury.[6–12] Recently many fluorescent mercury ionophores have been designed for Hg^{2+}-sensing such as calixarene,[13] hydroxyquinolines,[14,15] azines,[16] cyclams,[17–19] diazacrown ethers,[20] dioxocyclams,[21] diazatetrathia crown ethers,[22] and most of these studies have shown that nitrogen, oxygen, and sulfur atoms present in the ionophores can promote the coordination of Hg^{2+}.[16–22] However, some of these sensors have drawbacks in term of synthetic difficulty, high cost of starting materials or lack of selectivity and act generally in organic solvent, which limits their use in the real environmental mediums.

Usually the colorimetric and fluorescent chemosensors for the analytes detection contain generally binding sites and a signaling subunit that has the ability to display selective changes in absorption or fluorescence spectra upon guest binding. In this sense, it is reported that azathia macrocycle is generally thought to be a good receptor due to its strong ability to coordinate with heavy and transition metal ions such as Cu^{2+} and Hg^{2+} [23–25] and dansyl chloride is a classical fluorophore widely used in the development of fluorescent sensors due to its solvatochromism and high emission quantum yields.[26–28] Additionally, intramolecular charge transfer (ICT) is an effective signaling mechanism employed in the design of fluorescent sensors.[29–32] All these may be useful to develop new fluorescent sensors for Hg^{2+} in the environmental mediums.

On the other hand, hybrid organic/inorganic materials are widely used for many applications such as catalysis,[33] organic synthesis,[34] environment,[35] and electronics.[36] The anchoring of organic fractions on the surface of a silica material represents the key step for the development of new materials and can be mostly achieved using two approaches.[37] The first method consists in one-pot synthesis involving co-condensation reactions between an organo-tri-alkoxysilane and tetra-alkoxysilane (TEOS or TMOS) in the presence or absence of a molecular structure-directing agent

* Corresponding author. Tel.: +33 (0)320258687; fax: +33 (0)320272597; e-mail addresses: jalal.isaad@ensait.fr, jisaadjalal@gmail.com (J. Isaad).

0040-4020/$ – see front matter © 2013 Elsevier Ltd. All rights reserved.
http://dx.doi.org/10.1016/j.tet.2013.04.072

like a ionic or non-ionic surfactant. The second option consists of a functionalization of silanol groups on the surface of the material also called 'post-synthetic' functionalization method.

In particular, there are several advantages to using functionalized organic–inorganic hybrid nanomaterials as chemosensors in the environment. First, functionalized nanomaterials can rapidly and easily detect the metal ions.[38] Second, these nanomaterials would be useful as highly selective and efficient adsorbents for specific guest molecules in environmental pollutants due to the competition complex reaction. Third, the nanomaterials can be easily controlled to interact with target guest molecules for detection among various guest molecules in real analytical samples.

In this study, we selected a dansyl derivative as fluorophore with azathia crown ether moiety; the final fluorescent probe was supported on silica nanoparticles (**SiNPs**) as sophisticated hosts, for binding Hg^{2+}. The silica nanoparticles are particularly attractive as they are easy to synthesize, are aqueous solution friendly, and can be easily engineered to various sizes and shapes.

The methodology is showed in Scheme 1. First, the **SiNPs** were prepared by condensation of TEOS in the presence of DIW/EtOH and 30% aq ammonia solution. After the synthesis of the **SiNPs**, we were able to specifically modify the external surface of the **SiNTs** by using an adequate spacer such as aminopropyl-trimethoxysilane. By this process, the fluorophore-coupled azathia crown ether receptor **2f** was attached onto the surface of **SiNPs** as a chromogenic receptor for Hg^{2+}.

2. Results and discussions

2.1. Synthesis of the fluorophore 2f

Fluorescence signaling, which translates molecular recognition into tangible fluorescence signals, is one of the first choices due to its high detection sensitivity and simplicity. On the other hand, as well known, the sulfur and nitrogen can provide the soft binding unit for Hg^{2+} according to the hard–soft acid–base theory. The Hg^{2+} binding may affect intramolecular charge transfer (ICT) and consequently induce spectral change. The foregoing may be also applicable to the sensing of Hg^{2+}. With these in mind, an *ICT* fluorescent sensor **2f** based on azathia crown ether consisting of sulfur and nitrogen was designed and synthesized, which can selectively coordinate with Hg^{2+}. Scheme 1 reports the synthesis of the fluorophore **2f** and the azathia crown ether moiety **1d**.

In order to synthesize the fluorophore **2f**, the azathia crown ether **1d** was firstly synthesized from **1a** through three steps. As shown in Scheme 1A, bis (chloroethyl) amine **1a** was reacted with 2-mercaptoethanol under a basic condition using Na_2CO_3 as an inorganic base to afford the diol **1b**. Then, **1c** was prepared by the nucleophilic substitution of the diols groups of **1b** to their corresponding dichloro derivatives in the presence of $SOCl_2$. Finally, the azathia crown ether **1d** was obtained by the condensation of **1c** with 1,2-ethanedithiol under reflux and a basic condition. The prepared azathia crown ether **1d** was directly reacted with the

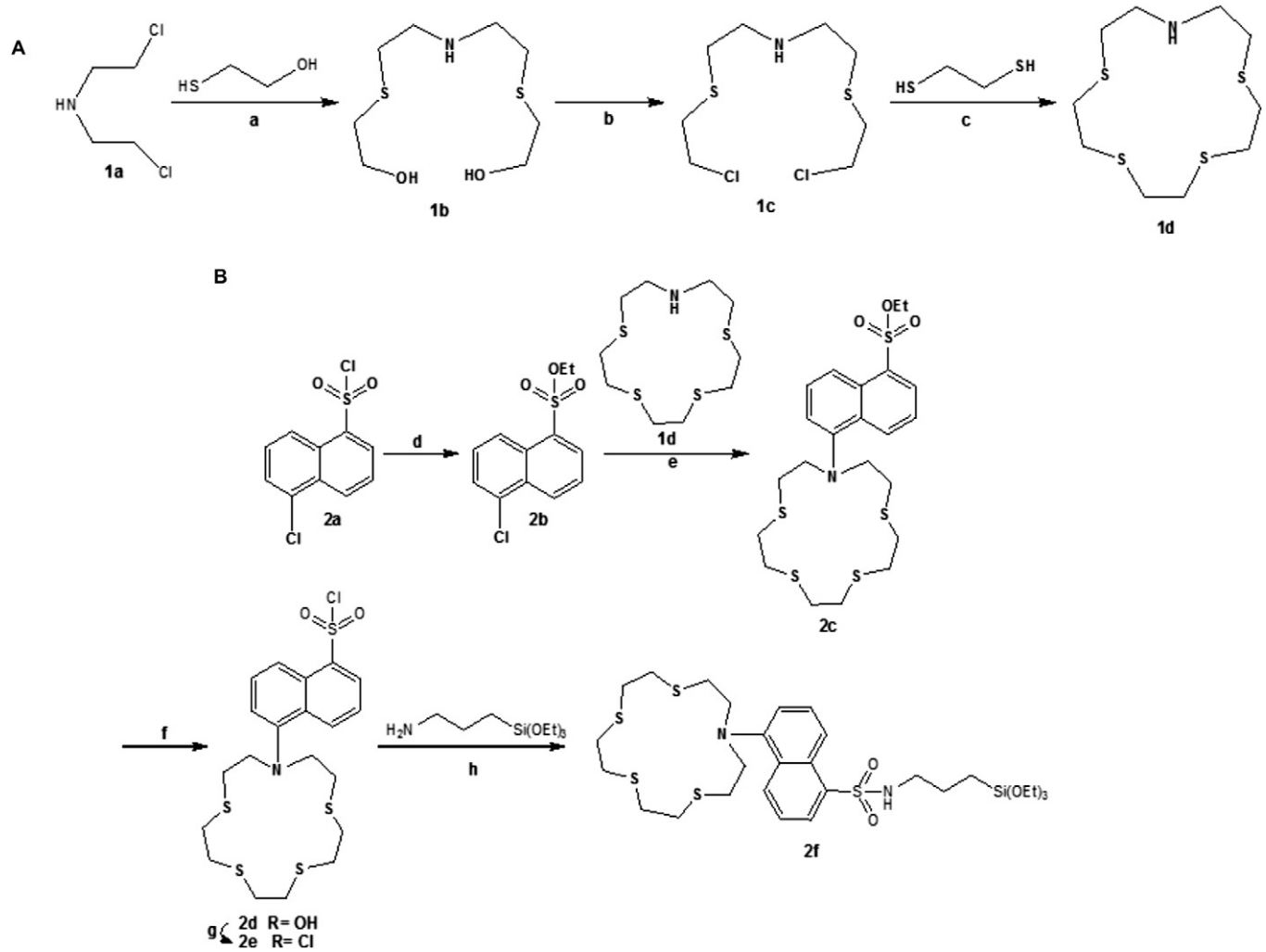

Scheme 1. Synthesis of the fluorophore **2f**. Reagent and conditions: (a) Na_2CO_3, THF/H_2O, 12h, 80 °C; (b) $SOCl_2$, DCM; (c) LiOH, THF, reflux, 3 days; (d) EtOH, rt, ultrasound (40 kHz), 30 min; (e) NEt_3, MeCN, reflux, 18 h; (f) NaOH, MeCN, rt, ultrasound (40 kHz), 20 min; (g) cyanuric chloride, acetone, 18-crown-6, reflux, 20 h; (h) NEt_3, DSM, 12 h, rt.

derivative **2b** in the presence of NEt_3 and under reflux for several hours to give **2c**. The esterification of the chlorosulfonate group of compound **2a** was carried out in EtOH and under ultrasound irradiation in order to favor the nucleophilic substitution reaction of the azathia crown ether **1d** with the chloro group in the *para*-position of the naphthalene moiety of **2a**. The fluorophore **2f** was obtained by the coupling of the aminopropyl-trimethoxysilane and compound **2e**, which prepared by the saponification and subsequently treated with cyanuric chloride. The structure of all derivatives was confirmed by MS, NMR, and elemental analysis.

2.2. Synthesis and characterization of the functionalized SiNPs

The study described here is based on design and development of a fluorescent optical sensor containing **SiNPs** functionalized with a metal ion chelating group. First, the **SiNPs** were prepared starting from TEOS in the presence of the absolute EtOH, DIW, and 30% aq ammonia solution. After, the surface of the prepared silica nanoparticles was modified by the fluorophore **2f** containing the organosilane moiety as shown in Fig. 1. The structural information of the

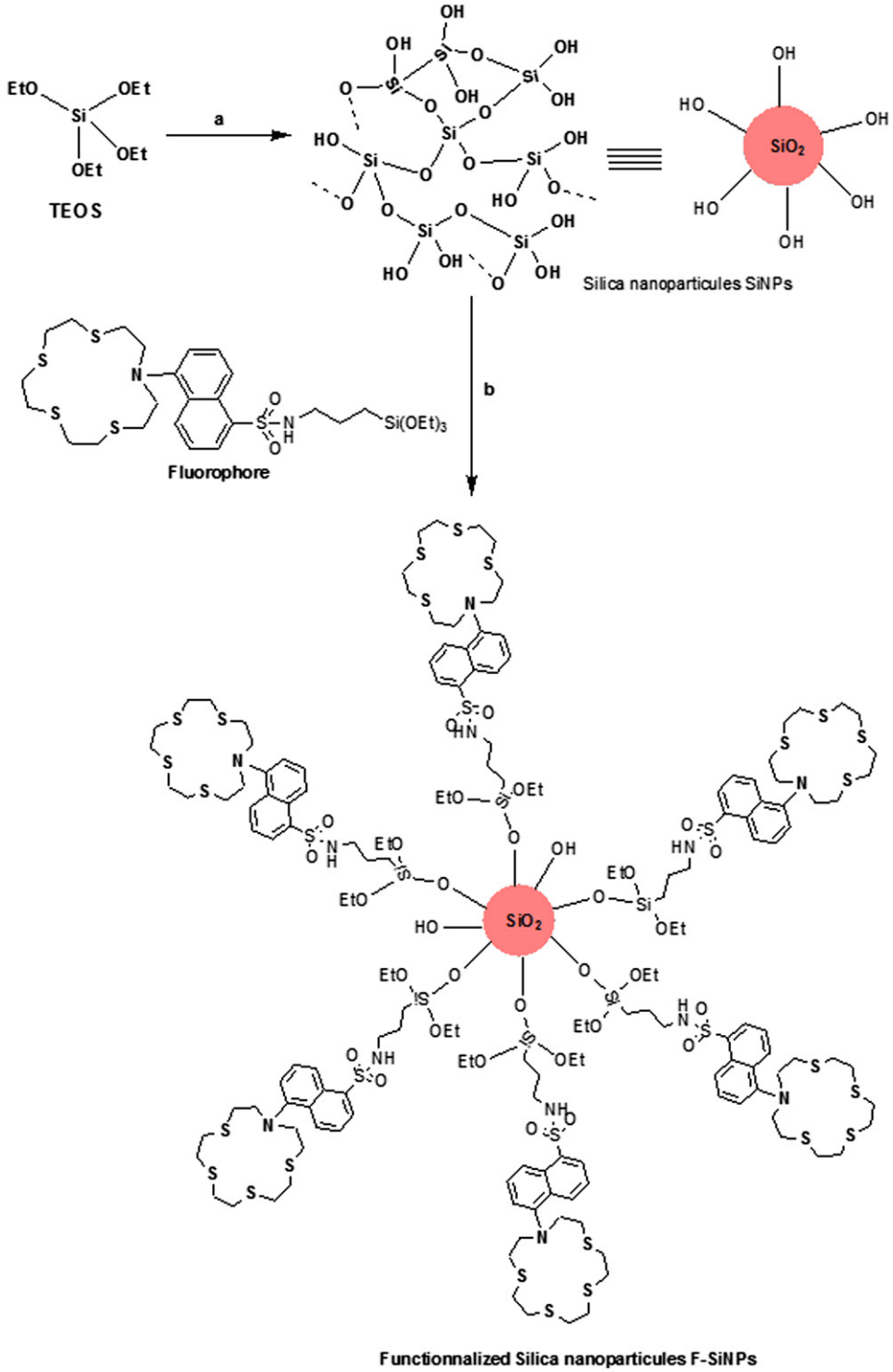

Fig. 1. General process for the synthesis of the functionalized silica nanoparticles (**F-SiNPs**). Reagents and conditions: (a) absolute EtOH, DIW/TEOS; sonicated for 2 h at 45 °C and 30% aq NH_3 solution was added and sonicated for 8 h at 45 °C; (b) anhyd toluene, Δ for 8 h.

fluorophore on the surface of silica nanoparticles was studied by solid-state characterization techniques: TEM imaging, TGA, and FTIR.

Thermal stability of the **SiNPs** and the functionalized **SiNPs** has been determined by thermogravimetric analysis. The results are shown in Fig. 2. The TGA weight loss curves for modified and unmodified **SiNPs** showed in Fig. 2 provide a qualitative comparison of the changes induced after modification. The unmodified **SiNPs** exhibit a weight loss at about 72 °C corresponding to the loss of physically adsorbed water, suggesting the surface to be hydrophilic in nature.[39] With increase in temperature the weight loss remains constant, indicating no appreciable condensation of silanol groups on the surface. There is a significant change in the weight loss curve with modification of **SiNPs**. As reported in the literature, the resulting pattern in the weight loss curve depends on the nature of the ligand, and the step transition shows the decomposition of the bonded organosilane with the height being roughly proportional to the carbon content. In Fig. 2, a major weight loss region is seen between 262 and 575 °C, indicative of decomposition of the organic ligand covalently bonded to the **SiNPs** surface.

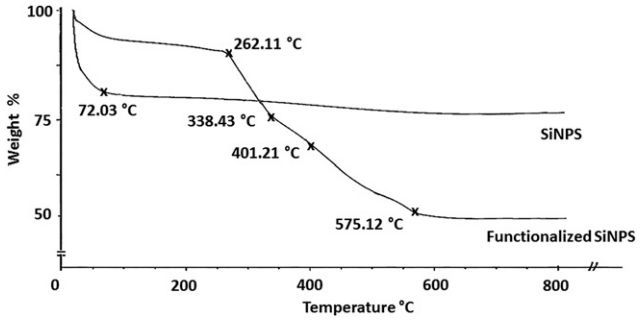

Fig. 2. TGA weight loss curves of unmodified **SiNPs** and modified **SiNPs**.

The amount of organic compounds bound on the surface of the nanoparticles is estimated from the percentage of weight loss from the TGA curve. TGA of the in **F-SiNPs** indicated that the fluorophore **2f** content was about 35%. Fluorophore **2f** started to decompose at about 262 °C and was completely burned out at about 575 °C.

The TEM images of the prepared **SiNPs** and the functionalized **SiNPs** used in this study are shown in Fig. 3. The **SiNPs** present a spherical shape with an average particle diameter of about 30 nm. When the **SiNPs** were functionalized with the fluorophore **2f**, the two undergo copolymerization, giving an aggregation of **SiNPs** in the range of 200 nm size particles, which comprises a network of irregular shaped **SiNPs** as shown in Fig. 3.

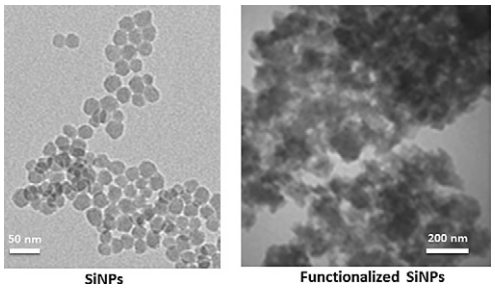

Fig. 3. TEM images of the unmodified and the functionalized **SiNPs**.

The modified **SiNPs** were also confirmed by FTIR analysis. The FTIR spectra of the modified and unmodified **SiNPs** are shown in Fig. 4. As reported in the spectrum A, the broad band at 3468 cm^{-1} represents the surface silanols of the unmodified **SiNPs**. The band at 1621 cm^{-1} represents the bending mode of *–OH* vibrations. The intense band centered at 1104 cm^{-1} is assigned to the structural *Si–O–Si* vibrations. The bands around 982 cm^{-1} resulted from *Si–O* vibrations. However, in the case of the functionalized **SiNPs**, in the FTIR spectrum (Fig. 4B), the silanol band disappears, whereas the *–NH* vibration band appears at 3264 cm^{-1}. The weak bands at 2694 cm^{-1} corresponding to the carbon chain (*CH*) of the pendant group attached to the inorganic matrix. Also, the band at 1531 cm^{-1} is attributed to the *C=C* aromatic stretch. The region between 1343 and 1489 cm^{-1} corresponds to the aliphatic *C–H* stretching and the *S=O* bands. These results showed that the fluorophore **2f** had been grafted onto the surface of the **SiNPs** after chemical modification.

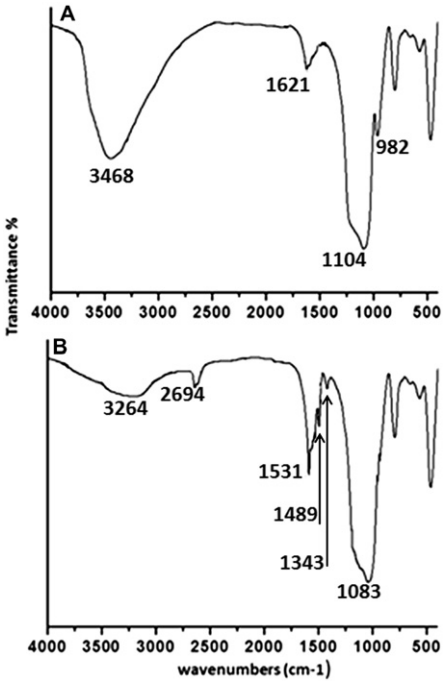

Fig. 4. FTIR spectra of unmodified **SiNPs** (A) and modified **SiNPs** (B).

2.3. Sensitivity studies of the functionalized SiNPS

The effects of water ratio on the fluorescence emission of the functionalized nanoparticles **F-SiNPs** in the absence and presence of metal ions were systematically investigated in ethanol solutions in order to optimize the conditions for practical applications in environmental and biological samples. Fig. 5 reports the effect of water ratio on the fluorescence behavior of **F-SiNPs** in ethanol solutions.

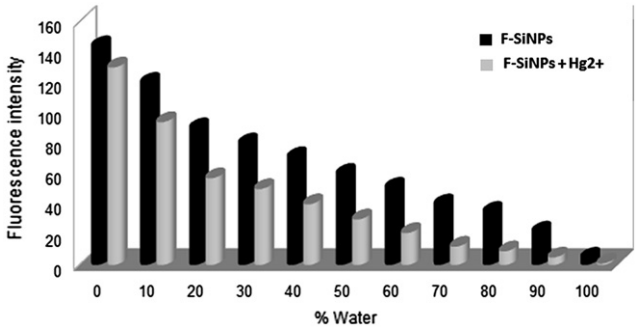

Fig. 5. The fluorescence intensity variations of the **F-SiNPs** (0.5 μM) as a function of the water ratio in ethanol solution at 525 nm in the absence and the presence of Hg^{2+} (5 equiv), λ_{ex} 340 nm.

The fluorescence emission of **F-SiNPs** was found to be strongly dependent on the presence of water in the aq ethanol solution. This result illustrated that when the water ratio increased, the fluorescence emission intensity of **F-SiNPs** decreased progressively. In the low water ratio range, a similar decrease in the response of **F-SiNPs** in the presence of 5 equiv of Hg^{2+} was observed, but with much larger changes compared to the high water ratio region. Following these results, we focused on the fluorescence behaviors of **F-SiNPs** in response to the different metal ions in 30:70 ethanol/water solution.

2.4. Selectivity study

As reported in the literature, the transition metal ions are well known as fluorescence quenchers and function by means of numerous mechanisms, such as fluorescence resonance energy transfer, electronic energy transfer, charge-transfer phenomena, heavy atom effects, magnetic perturbations, ground-state complexation, and collisional conversion of electronic to kinetic energy.[40] For an excellent chemosensor, high selectivity is a matter of necessity. For this purpose, the selectivity studies of **F-SiNPs** were performed in 30:70 ethanol/water solutions by recording the fluorescence spectra of the solutions of **F-SiNPs** after the addition of each representative metal ions. Fig. 6 shows the dependence of the fluorescence intensity **of F-SiNPs** as a function of cation concentrations for Hg^{2+}, transition metal, heavy metal, alkali earth, and alkali ions including K^+, Na^+, Ag^+, Ba^{2+}, Mg^{2+}, Ca^{2+}, Cd^{2+}, Co^{2+}, Cu^{2+}, Fe^{2+}, Fe^{3+}, Mn^{2+}, Ni^{2+}, Pb^{2+}, and Zn^{2+}. The selectivity studies clearly demonstrated the high selectivity of **F-SiNPs** to Hg^{2+} in comparison with the other cations. Only the addition of Hg^{2+} caused a dramatic decrease in the fluorescence spectra, while the other metal ions did not cause obvious changes under identical conditions. Furthermore, after addition of 5 equiv of Hg^{2+} to a solution of **F-SiNPs** in EtOH/H_2O: 30:70 mixture, a very noticeable decrease and also a blue shift fluorescence change were caused when excited by the radiation of 340 nm, which demonstrated **F-SiNPs** could selectively recognize Hg^{2+} by simple fluorescence chemosensing.

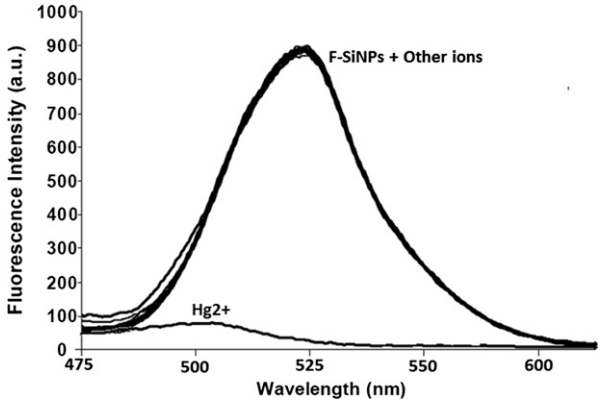

Fig. 6. Fluorescence spectra of **F-SiNPs** (1.0^{-5} M) in the presence of 5 equiv of different metal ions (Hg^{2+}, K^+, Na^+, Ag^+, Ba^{2+}, Mg^{2+}, Ca^{2+}, Cd^{2+}, Co^{2+}, Cu^{2+}, Fe^{2+}, Fe^{3+}, Mn^{2+}, Ni^{2+}, Pb^{2+}, and Zn^{2+}) in EtOH/H_2O: 30:70 mixture (λ_{ex} 340 nm).

To evaluate the quantitative binding affinity of **F-SiNPs**, the fluorescence titrations of **F-SiNPs** with increasing among of Hg^{2+} ions were carried out in 30:70 ethanol/water (Fig. 7).

Following Fig. 7, the **F-SiNPs** showed the maximum emission wavelength of 525 nm when excited by the radiation of 340 nm and has a high fluorescence quantum yield (ϕ=0.39). The fluorescence intensity of **F-SiNPs** was gradually decreased with increasing Hg^{2+} concentration. In the absence of Hg^{2+} ions, the fluorescence response was at a maximum and the response decreased as the

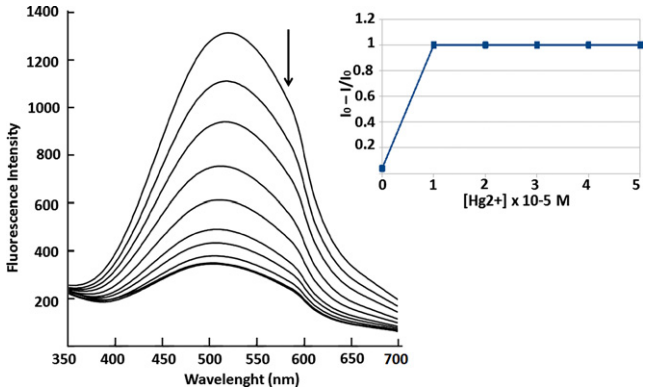

Fig. 7. Fluorescence emission spectra (λ_{ex} 340 nm) of **F-SINPs** (10^{-5} M) in 30:70 EtOH/H_2O as function of [Hg^{2+}] from 0.01 to 100 μM.

mercury concentration was increased. When the added mercury attained a concentration approximately more than three times higher than that of **F-SiNPs**, about 95% quenching of initial fluorescence of **F-SiNPs** was observed and the fluorescence response reached a minimum point. The result provided a proof for the formation of a new complex between Hg^{2+} and the fluorophore grafted on the **F-SiNPs**.

The Job's method for the emission was employed to investigate the binding stoichiometry of the **F-SiNPs** and Hg^{2+} ions. The total concentration of **F-SiNPs** and Hg^{2+} was maintained constant at 10^{-5} M, with a continuous variation of the molar fraction of Hg^{2+}. Fig. 8 shows the fluorescence intensity variation at 525 nm as a function of the ratio of **F-SiNPs**/Hg^{2+}concentration. Fig. 8 shows that the complex of **F-SiNPs**/Hg^{2+} exhibited a maximum fluorescence emission at 525 nm when the molecular fraction of Hg^{2+} was 0.5. This indicated that a 1:1 stoichiometry is most possible for the binding mode of **F-SiNPs** and Hg^{2+}.

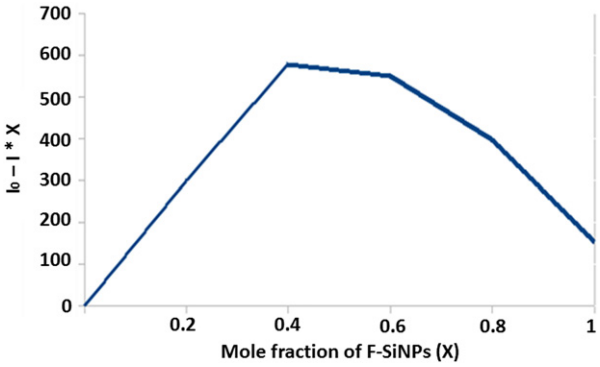

Fig. 8. Job's plot of **F-SiNPs**/Hg^{2+} system in 30:70 EtOH/H_2O. [**F-SiNPs**]+[Hg^{2+}]= 10^{-5} M.

2.5. pH effect on sensor

The performance characteristic of the sensor system was monitored for its sensitivity toward different pH conditions. It is essential for the sensor to perform satisfactorily at physiological pH for its application toward biological sensing. In this sense, the fluorophore grafted on the **F-SiNPs** presents nitrogen with lone pair electrons, the photophysical property of **F-SiNPs** and the sensing of Hg^{2+} might be influenced by the pH of the solution. Therefore, the response of the **F-SiNPs** toward Hg $^{2+}$ at different pH values is reported in Fig. 9. A 10^{-5} M stock solution of **F-SiNPs** containing 1 μM Hg^{2+} solution was used for the experiment and different pH solutions were prepared As reported in Fig. 9, in the absence of the Hg^{2+}

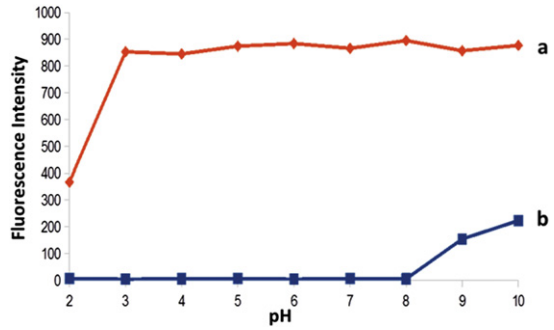

Fig. 9. Fluorescence emission response of **F-SiNPs** (10^{-5} M) at different pH (2–10), in the absence (a) and in the presence (b) of Hg^{2+} cations (1.0 μM) (λ_{ex} 340 nm).

ions, at pH<3.0, the fluorescence intensity decreased with decreasing pH value, which was caused by the protonation of the nitrogens of **F-SiNPs**.

Then, the fluorescence intensity of **F-SiNPs** almost did not vary with pH in the range from 3.0 to 10.0 in the mixed solution. Upon addition of Hg^{2+}, the fluorescence quenching almost did not cause changes in the range from 2.0 to 8.0 in mixed solution. When the pH was higher than 8.0, the fluorescence quenching was weakened because too high a pH would lead to formation of the precipitation of HgO, which in turn, would reduce its complexation with Hg^{2+}. The pH study shows that the **F-SiNPs** could be used as chemosensor for Hg^{2+} under pH ranged from 2 to 8, which covered the physiological pH condition.

The detection limit[41] of the **F-SiNPs** as a fluorescent sensor for the analysis of Hg^{2+} was determined from the plot of fluorescence intensity as a function of the Hg^{2+} concentration as reported in Fig. 10. The detection limit DL of chemosensor **F-SiNPs** was determined from the following equation:

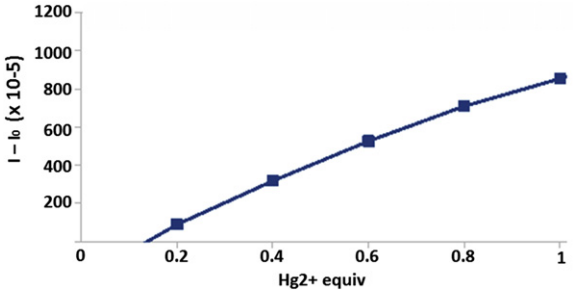

Fig. 10. Calibration curve of **F-SiNPS**/Hg^{2+} in EtOH/water: 30:70. The excitation wavelength was 340 nm.

$$DL = K \times Sb1/S$$

where: K=3; Sb1 is the standard deviation of the blank solution and S is the slope of the calibration curve.

It was found that the **F-SiNPs** have a detection limit of 10^{-7} M (see Supplementary data), which is allowed for the detection of micromolar concentration range of Hg^{2+}.

The association constant K_a was evaluated graphically by the plotting $1/\Delta F$ against $1/[Hg^{2+}]$ (Fig. 11).[42] The data were linearly fit according to the Benesi–Hilderbrand equation. The K_a value, obtained from the slope and intercept of the line, was found to be $2.9.10^3$ M^{-1}.

The effect of the different counterions on the sensor performance was also evaluated using different mercury salts such as NO_3^-, SO_4^{2-}, CH_3COO^-, CN^-, ClO_4^-, Cl^-, Br^-, and F^- at 1 μM as concentration. Fig. 12 shows the bar graph of the ratio of emission intensity of **F-SiNPs** with the different mercury salts. The maximum

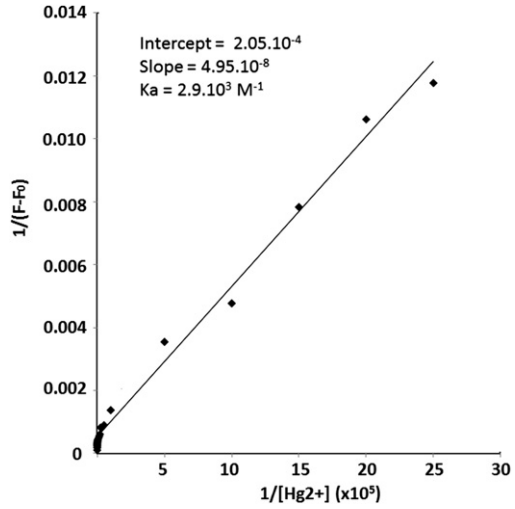

Fig. 11. Benesi–Hildebrand plot of the chemosensor **F-SiNPs**/Hg^{2+} complexes in EtOH/water: 30:70.

emission intensity was observed in case of $HgCl_2$ and $HgBr_2$, and the minimum emission intensity was observed in case of $HgCN_2$. Overall, the effect of different counterions on the sensor system, as compared with the chloride counterion used this work, is not more than 5%.

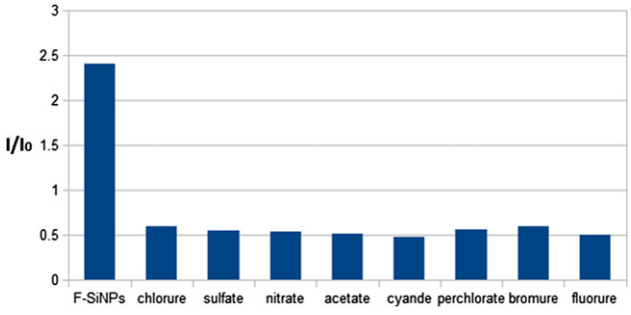

Fig. 12. Bar graph of ratio of fluorescence emission intensity, of **F-SiNPs** (10^{-5} M) with different mercury ions at 1 μM of concentration.

3. Conclusions

A novel fluorometric sensor has been developed using functionalized silica nanoparticles for sensitive and selective detection of Hg^{2+} in aqueous suspension. A derivative of dansyl with azathia crown ether moiety was used as fluorophore and metal ions chelator to functionalize the silica nanoparticles. The results of fluorescence experiments exhibited a pronounced Hg^{2+} selective ON–OFF type fluorescence switching upon binding. The detection limit of 10^{-7} M Hg^{2+} in EtOH/H_2O at neutral pH is observed. The presence of other metal ions does not affect the selectivity of the sensor, even in the presence of high concentrations 5.10^{-5} M of Hg^{2+}, K^+, Na^+, Ag^+, Ba^{2+}, Mg^{2+}, Ca^{2+}, Cd^{2+}, Co^{2+}, Cu^{2+}, Fe^{2+}, Fe^{3+}, Mn^{2+}, Ni^{2+}, Pb^{2+}, and Zn^{2+}. This sensor shows selective detection of Hg^{2+} and can be used for Hg^{2+} chemosensing in physiological environment and water quality monitoring.

4. Experimental section

4.1. Materials and instrumentation

All chemicals were reagent grade (Aldrich Chemical Co.) and were used as purchased without further purification. Thin layer chromatography (TLC) analysis was performed using Fluka

aluminum foils coated with 25 mm particle size silica gel matrix F_{254}. TLC development involved either UV (254 and 366 nm) or visible light inspection, followed by either treatment with an acid solution of *p*-anisaldehyde or a basic solution of $KMnO_4$ and heating. Flash column chromatography was performed on Merck silica gel 60 (particle size 0.040–0.063 nm, 230–400 mesh ASTM) according to the procedure of Still. UV–vis spectra were recorded on a Cary-4000 Varian spectrophotometer, using either 0.1 or 1 cm quartz cuvettes. Infrared spectra were recorded in a KBr disk on a Perkin Elmer-Spectrum BX FTIR system. Absorptions are quoted in wavenumbers (cm^{-1}). ^1H and ^{13}C NMR spectra were recorded at 200 MHz (for the ^1H) and 50.0 MHz (for the ^{13}C) on a Varian Gemini spectrometer. Spin resonances are reported as chemical shifts (δ) in parts per million (ppm) and referenced to the residual peak as an internal standard of the solvent employed, as follow: $CDCl_3$ 7.27 ppm (^1H NMR), 77 ppm (^{13}C NMR, central band), DMSO-d_6 2.50 ppm (^1H NMR, central band), 39.5 ppm (^{13}C NMR, central band). Spin multiplicity is showed by s=singlet, d=doublet, t=triplet, q=quartet, m=multiplet, br=broad. Coupling constants *J* are reported in hertz (Hz). Mass spectra were recorded on a ThermoScientific LCQ-Fleet mass spectrometer under electrospray ionization (ESI, +c or −c technique). High-resolution mass spectra (HRMS) were recorded on a LTPOrbitrap mass spectrometer from Thermo Electron Corporation under ESI (+c) technique. Mass spectrometric analysis is quoted in the *m*/*z* form. Elemental analyses were recorded on a Perkin Elmer 240 C Elemental Analyzer. The fluorescence spectra were measured by Hitachi F-4500 fluorescence spectrophotometer with a 1 cm quartz cell. Doubly distilled deionized water (DIW) was used for all experiments.

4.2. Synthesis of 5-chloro-naphthalene-1-sulfonic acid ethyl ester (2b)

A solution of **2a** (1.00g, 3.84 mmol) was dissolved in EtOH (7 mL), and the mixture was irradiated at rt in the water bath of an ultrasonic cleaner for 30 min. Then, the solvent was removed under reduce pressure, the crude was washed with water and DCM. The resulting residue was dried under reduced pressure to afford **2b** in quantitative yield. H NMR (DMSO-d_6, 200 MHz): δ=8.49–8.16 (m, 2H, Ar*H*), 7.51–7.22 (m, 4H, Ar*H*), 3.77 (q, 2H, *J*=8.4 Hz, CH_2), 1.38 (t, 3H, *J*=8.4 Hz, CH_3) ppm. ^{13}C NMR (d6- DMSO, 50 MHz): δ=141.2, 132.5, 131.8, 130.4, 128.3, 127.3, 126.7, 126.1, 125.5, 124.9, 52.3, 13.3 ppm. MS (ESI): *m*/*z*=271.36 $[M+1]^+$. $C_{12}H_{11}ClO_3S$ (270.01): C, 53.24; H, 4.10. Found: C, 53.33; H, 4.21.

4.3. 5-(1,4,7,10-Tetrathia-13-aza-cyclopentadec-13-yl)-naphthalene-1-sulfonic acid ethyl ester (2c)

MeCN solution (15 mL) was added to a 100-mL round bottom flask containing the azatha crown ether **1d** (0.5 g, 1.76 mmol), compound **2b** (0.48 g, 1.76 mmol), and NEt_3 (0.74 g, 5.28 mmol), the mixture was stirred under reflux for 18 h under a nitrogen atmosphere. After completion of the reaction (which was monitored by TLC), MeCN was removed from the mixture under reduced pressure. The resulting crude product was purified by silica gel column chromatography using EtOAc/PE (5:2) to yield compound **2c** in 35% as yield. H NMR (DMSO-d_6, 200 MHz): δ=8.12–7.56 (m, 3H, ArH), 7.21–6.66 (m, 3H, ArH), 3.77 (t, 4H, *J*=8.1 Hz, NCH_2), 3.51 (q, 2H, *J*=7.8 Hz, CH_2), 2.91–2.88 (m, 12H, CH_2), 2.63 (t, 4H, *J*=8.1 Hz, NCH$_2$CH_2), 1.36 (t, 3H, *J*=7.8 Hz, CH_3) ppm. ^{13}C NMR (DMSO-d_6, 50 MHz): δ=152.5, 141.5, 131.9, 130.3, 128.2, 127.4, 125.3, 124.4, 122.3, 115.2, 58.3, 54.1, 34.7, 34.2, 31.2, 13.3 ppm. MS (ESI): *m*/*z*=518.29 $[M+1]^+$. $C_{22}H_{31}NO_3S_5$ (517.08): C, 51.03; H, 6.03; N, 2.70. Found: C, 51.18; H, 6.21; N, 2.84.

4.4. 5-(1,4,7,10-Tetrathia-13-aza-cyclopentadec-13-yl)-naphthalene-1-sulfonyl chloride (2e)

To a solution of compound **2c** (0.5 g, 0.97 mmol) in MeCN (15 mL), 2 mL of NaOH solution 1 N was added and the mixture was irradiated at rt in the water bath of an ultrasonic cleaner for 20 min. Then the solvent was removed under reduced pressure and the crude was washed with DCM, and the residue was dried under pressure to afford the corresponding sodium sulfonate derivative **2d**. After, this hydrolysis of compound **2c**, the derivative **2d** was dissolved in 20 mL of acetone and 5 mL of cyanuric chloride was added with a catalytic quantity of 18-crown-6 ether and the resulting mixture was heated under reflux for 20 h. After cooling to rt the solution was filtered through a Celite. Solvent was removed (rotary evaporator) and the sulfonyl chloride was purified by FCC using EtOAc/PE (5:2) as eluent to yield compound **2e** in 75% as yield. H NMR (DMSO-d_6, 200 MHz): δ=8.11–7.54 (m, 3H, ArH), 7.31–6.68 (m, 3H, ArH), 3.76 (t, 4H, *J*=8.5 Hz, NCH_2), 2.91–2.87 (m, 12H, CH_2), 2.65 (t, 4H, *J*=8.4 Hz, NCH$_2$CH_2) ppm. ^{13}C NMR (DMSO-d_6, 50 MHz): δ=152.1, 144.2, 134.3, 131.3, 130.4, 126.8, 125.9, 124.6, 123.4, 114.7, 58.2, 34.6, 34.3, 31.5 ppm. MS (ESI): *m*/*z*=507.03 $[M+1]^+$. $C_{20}H_{26}ClNO_2S_5$ (508.31): C, 47.27; H, 5.16; N, 2.76. Found: C, 47.35; H, 5.28; N, 2.86.

4.5. Synthesis of the compound 2f

In an ice bath, a solution of **2e** (0.5 g, 0.98 mmol) in 15 mL of DCM was added slowly to a mixture of aminopropyltrimethoxysilane and triethylamine in DCM (30 ml) and then was stirred for 0.5 h. The reaction mixture was kept stirring for 12 h at rt, and the progress of the reaction was monitored by thin layer chromatography (TLC). After dilution with DCM, the mixture was washed with saturated brine. The organic phase was dried over anhydrous $MgSO_4$, filtered, and evaporated under reduced pressure. Purification of **2f** was performed by using column chromatography on silica gel using MeOH/DCM: 1:10 as eluent afford **2f** in 68% as yield. H NMR (DMSO-d_6, 200 MHz): δ=8.03–7.56 (m, 3H, ArH), 7.21–6.63 (m, 3H, ArH), 3.89 (m, 6H, SiOCH_2), 3.71 (t, 4H, *J*=8.1 Hz, NCH_2), 3.11 (t, 2H, *J*=6.9 Hz, CH_2N), 2.93–2.87 (m, 12H, CH_2), 2.65 (t, 4H, *J*=7.6 Hz, NCH$_2$CH_2), 1.56–1.23 (m, 11H), 0.63 (t, 2H, *J*=6.4 Hz, SiCH_2) ppm. ^{13}C NMR (DMSO-d_6, 50 MHz): δ=152.8, 139.3, 132.6, 130.6, 128.5, 126.6, 125.5, 124.1, 123.2, 114.5, 58.6, 51.1, 43.3, 35.1, 34.2, 31.4, 17.1, 15.6, 9.1 ppm. MS (ESI): *m*/*z*=693.36 $[M+1]^+$. $C_{29}H_{48}N_2O_5S_5Si$ (692.19): C, 50.25; H, 6.98; N, 4.04. Found: C, 50.35; H, 7.11; N, 4.16.

4.6. Synthesis of 2-{2-[2-(2-hydroxy-ethylsulfanyl)-ethyl-amino]-ethylsulfanyl}-ethanol (1b)

To a 50 mL reactor were added sodium carbonate (1.0 g, 8.98 mmol), tetrahydrofuran (15 mL), water (2 mL), and compound **1a** (1.0 g, 6.95 mmol). The reaction mixture was flushed with nitrogen for 20 min, and then 2-mercaptoethanol (0.99 mL, 13.9 mmol) was added in one portion. The reaction mixture was stirred for 12 h at 80 °C under nitrogen atmosphere. The reaction mixture was diluted with water (20 mL) and extracted with dichloromethane (5×50 mL). The combined organic phase was dried over $MgSO_4$. After filtration, the filtrate was condensed to dryness. The residue was purified by column chromatography (EtOAc/PE, 4:1, v/v) to afford **1b** in 32.0% as yield. H NMR (DMSO-d_6, 200 MHz): δ=3.88 (t, 4H, *J*=7.7 Hz, OCH_2), 2.91 (t, 4H, *J*=6.7 Hz, NCH_2), 2.63–2.58 (m, 8H) ppm. ^{13}C NMR (DMSO-d_6, 50 MHz): δ=66.7, 50.6, 35.1, 34.8 ppm. MS (ESI): *m*/*z*=226.32 $[M+1]^+$. $C_8H_{19}NO_2S_2$ (225.09): C, 42.63; H, 8.50; N, 6.21. Found: C, 42.72; H, 8.64; N, 6.32.

4.7. Synthesis of bis-[2-(2-chloro-ethylsulfanyl)-ethyl]-amine (1c)

To a solution of compound **1b** (1 g, 4.44 mmol) in 15 mL of DCM, a solution of thionyl chloride (049 g, 4.44 mmol) was added dropwise to the above solution and stirred at −4 to 6 °C for 1 h. After the reaction mixture was placed at rt to react for 4 h and was heated to 60 °C to react for 5 h. The reactant was then washed with chloroform and purified by FCC (MeOH/DCM: 6:1) to afford **1c** (81%, R_f=0.65). H NMR (DMSO-d_6, 200 MHz): δ=3.77 (t, 4H, J=7.2 Hz, ClCH_2), 2.91 (t, 4H, J=6.3 Hz, NCH2), 2.69–2.57 (m, 8H) ppm. ^{13}C NMR (d6- DMSO, 50 MHz): δ=50.3, 48.2, 35.4, 34.3 ppm. MS (ESI): m/z=263.28 $[M+1]^+$. $C_8H_{17}Cl_2NS_2$ (261.02): C, 36.64; H, 6.53; N, 5.34. Found: C, 36.72; H, 6.63; N, 5.43.

4.8. Synthesis of 1,4,7,10-tetrathia-13-aza-cyclopentadecane (1d)

To a solution of **1c** (1 g, 3.81 mmol), ethane-1,2-dithiol (0.56 g, 3.81 mmol) and lithium hydroxide (94 mg, 3.81 mmol) in 15 mL of absolute tetrahydrofuran and the resulting mixture was refluxed under a nitrogen atmosphere for 3 days. The reaction mixture was filtered and then concentrated at reduced pressure. The residue was extracted three times with chloroform and the extract was washed with water. The solvent was removed after drying over anhydrous sodium sulfate. The crude product was purified by FCC (MeOH/DCM: 1:12, R_f=0.57) to give **1d** in 53% as yield. H NMR (DMSO-d_6, 200 MHz): δ=2.93–2.88 (m, 16H), 2.55 (t, 4H, J=6.7 Hz, NCH_2) ppm. ^{13}C NMR (DMSO-d_6, 50 MHz): δ=50.8, 35.5, 34.8, 34.2 ppm. MS (ESI): m/z=284.32 $[M+1]^+$. $C_{10}H_{21}NS_4$ (283.06): C, 42.36; H, 7.47; N, 4.94. Found: C, 42.44; H, 7.53; N, 5.12.

4.9. Fluorescence studies for metal ion detection

Each detection of metal ion was measured in 0.01 M H_2O/EtOH: 70:30 at pH 7. The stock solution of functionalized **SiNPs** was prepared in DIW (15.0 mg/2.0 mL). The concentration of the **SiNPs** in the test solutions for fluorescence measurements was kept at a constant value of 10^{-5} M. Stock solutions of 0.1 M concentration of $ZnCl_2$, NaCl, KCl, $CaCl_2$, $MgCl_2$, $MnCl_2$, $FeCl_2$, $FeCl_3$, $CuCl_2$, $CoCl_2$, $NiCl_2$, $CdCl_2$, $HgCl_2$, $PbCl_2$, and AgCl were prepared in DIW. Necessary dilutions were made according to each experimental set up. All fluorescence spectra were recorded at 22 °C with the excitation wavelength of 340 nm.

4.10. Synthesis of unmodified SiNPs

Absolute ethanol (15 ml) and DIW (25 ml) mixture was sonicated for 15 min followed by the addition of TEOS (15 mL; 0.066 mol). The mixture was sonicated for 2 h at 45 °C. After 28–30% aq ammonia solution (9.0 mL, 0.144 mol) was added to the above reaction mixture at a feed rate of 0.03 mL/min, after which time, the reaction mixture was sonicated further for 8 h at 45 °C. The **SiNPs** were separated and washed with 80% EtOH/DIW solution three times using centrifugation (11,200 *g* for 10 min) technique and cured at 110 °C for 24 h yielding 3.82 g of white silica NPs.

4.11. Determination of silanol concentration

The concentration of silanol groups on **SiNPs** surface was calculated through alkali neutralization method (Eq. 1) as reported in the literature.[43] *W* g (0.27 g) of the prepared **SiNPs** was mixed with 50 mL of 0.05 M aq solution of NaOH in a 100 mL conical flask. The flask was sealed and then stirred for 12 h. The mixture was centrifuged (16,128 *g* for 30 min) and 10 mL of supernatant was collected and titrated against standardized 0.05 M aq HCl (*A* ml) using 0.1% phenolphthalein as indicator. The above procedure was repeated with blank solution. The amount of HCl solution consumed for neutralization was designated as *B* mL. The reading for *A* and *B* were collected from the average of three titration experiments. The amount of total hydroxyl groups (*X* mmol g^{-1}) per unit gram of the silica was estimated (X=1.82 mmol g) according to the following Eq. 1.

$$X = \frac{(B-A)\times 0.005\times 5}{W} \quad (1)$$

4.12. Surface functionalization of SiNPs with the fluorophore 2f

In a round bottom flask, 250.0 mg (0.44 mmol) of **SiNPs** was suspended in a solution of 25.0 mL of anhydrous toluene and 0.08 mL DIW, and sonicated for 30 min at rt. The silane **2f** (0.47 g; 0.68 mmol) was hydrolyzed in 25.0 mL of anhydrous toluene and 0.12 mL DIW for 15 min at rt then added to **SiNPs** suspension and sonicated again for 30 min. The reaction mixture was refluxed for 24 h without magnetic stirring. The functionalized **SiNPs** were separated and washed twice with 90% toluene/DIW and 80% EtOH/DIW using centrifugation (11,200 *g* for 10 min) technique. Finally, the functionalized **SiNPs** were dried under vacuum at 110 °C for 24 h before use.

Supplementary data

Supplementary data associated with this article can be found in the online version, at http://dx.doi.org/10.1016/j.tet.2013.04.072.

References and notes

1. Renzoni, A.; Zino, F.; Franchi, E. *Environ. Res.* **1998**, *77*, 68.
2. Hardy, S.; Jones, P. *J. Chromatogr., A* **1997**, *791*, 333.
3. Harris, H. H.; Pickering, I. J.; George, G. N. *Science* **2003**, *301*, 1203.
4. Gutknecht, J. *J. Membr. Biol.* **1981**, *61*, 61.
5. Tchounwou, W.; Ayensu, K.; Ninashvili, N.; Sutton, D. *Environ. Toxicol.* **2003**, *18*, 149.
6. Singh, A. K.; Bhattacharjee, G.; Singh, R. *Sens. Actuators, B* **2004**, *99*, 36.
7. Guo, X.; Qian, X.; Jia, L. *J. Am. Chem. Soc.* **2004**, *126*, 2272.
8. Talanova, G. G.; Elkarim, N. S. A.; Talanov, V. S.; Bartsch, R. A. *Anal. Chem.* **1999**, *71*, 3106.
9. Shiraishi, Y.; Sumiya, S.; Kohno, Y.; Hirai, T. A. *J. Org. Chem.* **2008**, *73*, 8571.
10. Soh, J. H.; Swamy, K. M. K.; Kim, S. K.; Kim, S. H.; Lee, S. H.; Yoon, J. *Tetrahedron Lett.* **2007**, *48*, 5966.
11. Wang, F.; Peng, R.; Sha, Y. *Molecules* **2008**, *13*, 922.
12. Peng, R.; Wang, F. *Molecules* **2007**, *12*, 1191.
13. Metivier, R.; Leray, I.; Valeur, B. *Chem.—Eur. J.* **2004**, *10*, 4480.
14. Moon, S. Y.; Cha, N. R.; Kim, Y. H.; Chang, S. K. *J. Org. Chem.* **2004**, *69*, 181.
15. Zhang, H.; Han, L. F.; Zachariasse, K. A.; Jiang, Y. B. *Org. Lett.* **2005**, *7*, 4217.
16. Martinez, R.; Espinosa, A.; Tarraga, A.; Molina, P. *Org. Lett.* **2005**, *7*, 5869.
17. Kim, S. H.; Kim, J. S.; Park, S. M.; Chang, S. K. *Org. Lett.* **2006**, *8*, 371.
18. Park, S. M.; Kim, M. H.; Choe, J. I.; No, K. T.; Chang, S. K. *J. Org. Chem.* **2007**, *72*, 3550.
19. Moon, S. Y.; Youn, N. J.; Park, S. M.; Chang, S. K. *J. Org. Chem.* **2005**, *70*, 2394.
20. Kim, J. H.; Hwang, A. R.; Chang, S. K. *Tetrahedron Lett.* **2004**, *45*, 7557.
21. Song, K. C.; Kim, M. H.; Kim, H. J.; Chang, S. K. *Tetrahedron Lett.* **2007**, *48*, 7464.
22. Kim, S. H.; Song, K. C.; Ahn, S.; Kang, Y. S.; Chang, S. K. *Tetrahedron Lett.* **2006**, *47*, 497.
23. Lee, S. J.; Jung, J. H.; Seo, J.; Yoon, I. I.; Park, K. M.; Lindoy, L. Y.; Lee, S. S. *Org. Lett.* **2006**, *8*, 1641.
24. Sancenón, F.; Martínez-Màñez, R.; Soto, J. *Angew. Chem., Int. Ed.* **2002**, *41*, 1416.
25. Grant, G. J.; Botros, M. E.; Hassler, J. S.; Janzen, D. E.; Grapperhaus, C. A.; O'Toole, M. G.; VanDerveer, D. G. *Polyhedron* **2008**, *27*, 3097.
26. Dhir, A.; Bhalla, V.; Kumar, M. *Org. Lett.* **2008**, *10*, 4891.
27. Da, H.; Liu, F.; Gao, Q.; Fu, T.; Kou, X. *Luminescence* **2011**, *26*, 523.
28. Lee, M. H.; Kim, H. J.; Yoon, S.; Park, N.; Kim, J. S. *Org. Lett.* **2008**, *10*, 213.
29. Wang, J. B.; Qian, X. H.; Cui, J. N. *J. Org. Chem.* **2006**, *71*, 4308.
30. Xu, Z. C.; Xiao, Y.; Qian, X. H.; Cui, J. N. *Org. Lett.* **2005**, *7*, 889.
31. Yang, J. S.; Lin, Y. D.; Wang, S. S. *J. Org. Chem.* **2005**, *70*, 6066.
32. Mei, Y. J.; Bentley, P. A. *Bioorg. Med. Chem. Lett.* **2006**, *16*, 3131.
33. Corma, A. *Chem. Rev.* **1997**, *97*, 2373.
34. Polshettiwar, V.; Varma, R. S. *Tetrahedron* **2008**, *64*, 4637.
35. Newman, J. D. S.; Roberts, J. M.; Blanchard, G. J. *Anal. Chem.* **2007**, *79*, 3448.

36. Toyama, T.; Ichihara, T.; Yamaguchi, D.; Okamoto, H. *Appl. Surf. Sci.* **2007**, 254295.
37. Hoffmann, F.; Cornelius, M.; Morell, J.; Fröba, M. *Angew. Chem., Int. Ed.* **2006**, *45*, 3216.
38. Ros-Lis, J. V.; Casasffls, R.; Comes, M.; Coll, C.; Marcos, M. D.; Martinez-Manez, R.; Sancenon, F.; Soto, J.; Amoros, P.; El Haskouri, J.; Garro, N.; Rurack, K. *Chem. —Eur. J.* **2008**, *14*, 8267.
39. Jaroniec, C. P.; Gilpin, R. K.; Jaroniec, M. J. *J. Phys. Chem. B* **1997**, *101*, 6861.
40. Rupcich, N.; Chiuman, W.; Nutiu, R.; Mei, S.; Flora, K. K.; Li, Y.; Brennan, J. D. *J. Am. Chem. Soc.* **2006**, *128*, 780.
41. Zhu, M.; Yuan, M.; Liu, X.; Xu, J.; Lv, J.; Huang, C.; Liu, H.; Li, Y.; Wang, S.; Zhu, D. *Org. Lett.* **2008**, *10*, 1481.
42. Bourson, J.; Pouget, J.; Valeur, B. *J. Phys. Chem.* **1993**, *97*, 4552.
43. Rahman, I. A.; Vejayakumaran, P.; Sipaut, C. S.; Ismail, J.; Bakar, M. A.; Adnam, R.; Chee, C. K. *Colloids and Surfaces A: Physicochem. Eng. Aspects* **2007**, *294*, 102.